

Coulomb energy spacing is 50 meV (assuming that the oxide layer between the dot and channel is 1 nm thick) (6); (ii) because the barrier layer is thin, the voltage drop between the channel and the floating gate is very small; and (iii) once an electron is added to the floating gate, the potential of the floating gate rises, further reducing the voltage difference between the channel and the floating gate and preventing another electron from tunneling into the floating gate. Therefore, for a fixed charging voltage, the charging process is self-regulated and stops once the floating gate is charged with a fixed number of electrons, leading to a threshold shift independent of charging time and a staircase relation between the charging voltage and the threshold shift.

The discrete threshold shift is not a result of interfacial traps. The threshold shifts due to the traps will not be equally spaced (because the charge will be trapped at different locations of the channel), and the charging process will be time dependent (7).

Despite the small floating gate and the low level of channel doping, the device has a good subthreshold slope of 108 mV per decade, because the inversion layer induced by the control gate effectively acts as an ultrashallow source and drain for the device. This characteristic is also attributable to the low source and drain voltage.

As indicated by Eq. 1, the threshold voltage can be much larger than the present 55 mV if the thickness of the control gate oxide is increased or the fringing gate capacitance can be reduced. Also, if a thicker tunnel oxide is used between the channel and the floating gate, the charge on the floating gate can be held much longer than the current 5 s.

The SEMM should be investigated more thoroughly before being put into manufacturing. One of the most important questions to be studied is the effects of variations of

device size and stray charges on the threshold voltage. Nevertheless, the SEMM presented here is orders of magnitude smaller than the conventional floating gate MOS memory, has properties that conventional memories do not have, and is a major step forward in taking advantage of single electron effects to build ultrasmall and ultrahigh density transistor memories.

## REFERENCES AND NOTES

1. K. Yano *et al.*, *IEEE Trans. Electron Devices* **41**, 1628 (1994).
2. S. Tiwari *et al.*, *Appl. Phys. Lett.* **68**, 1377 (1996).

3. S. Y. Chou, unpublished results.
4. P. B. Fischer and S. Y. Chou, *Appl. Phys. Lett.* **62**, 2989 (1993); *J. Vac. Sci. Technol. B* **11**, 2524 (1993); E. Leobandung, L. Guo, S. Y. Chou, *ibid.* **13**, 2865 (1995).
5. H. I. Liu, D. K. Biegelsen, F. A. Ponce, N. M. Johnson, R. F. W. Pease, *Appl. Phys. Lett.* **64**, 1383 (1994).
6. The capacitance between the floating gate and the channel was calculated by the image charge method.
7. See, for example, J. R. Davis, *Instabilities in MOS Devices* (Gorden and Breach, New York, 1980).
8. This work was partially supported by the Defense Advanced Research Projects Agency, the Office of Naval Research, the Army Research Office, and the National Science Foundation.

21 October 1996; accepted 27 November 1996

## Micropatterning Fluid Lipid Bilayers on Solid Supports

Jay T. Groves, Nick Ulman, Steven G. Boxer\*

Lithographically patterned grids of photoresist, aluminum oxide, or gold on oxidized silicon substrates were used to partition supported lipid bilayers into micrometer-scale arrays of isolated fluid membrane corrals. Fluorescently labeled lipids were observed to diffuse freely within each membrane corral but were confined by the micropatterned barriers. The concentrations of fluorescent probe molecules in individual corrals were altered by selective photobleaching to create arrays of fluid membrane patches with differing compositions. Application of an electric field parallel to the surface induced steady-state concentration gradients of charged membrane components in the corrals. In addition to producing patches of membrane with continuously varying composition, these gradients provide an intrinsically parallel means of acquiring information about molecular properties such as the diffusion coefficient in individual corrals.

The patterning of surfaces into defined regions of contrasting properties has recently received considerable attention. Successes in this field include the development of micrometer-scale patterns in surface wettability (1) and microcontact printing, which has produced patterned self-assembled monolayers with submicrometer features (2, 3). At the same time, light-directed synthesis has been used to generate spatially addressable combinatorial libraries of DNA and protein sequences on solid substrates (4). Here, we describe patterning of surfaces with properties resembling those of living cells: fluid bilayer membranes on solid supports. This work has been stimulated by the desire to create integrated devices capable of manipulating molecules in a bilayer membrane and to pattern spatially addressable libraries of chemically distinct, fluid membrane patches.

Supported membranes are self-assembling, two-dimensional (2D) fluid systems

(Fig. 1). The bilayer membrane consists of two opposed leaflets of phospholipid molecules and is the basic structure central to all living cell membranes. Bilayers on solid supports were originally developed for studies of interactions between living cells, where they have proven highly useful (5, 6). Supported membranes can be formed by spontaneous fusion of lipid bilayer vesicles with an appropriate hydrophilic surface such as oxidized Si (7, 8). Interactions between membranes and surfaces involve electrostatic and hydration forces as well as attractive contributions from long-range van der Waals forces. An energetic minimum tightly traps the membrane near the surface. Supported bilayers are typically separated from the solid substrate by a thin (~10 Å) film of water (9–11) and retain many of the properties of free membranes, including lateral fluidity. The fluidity is long range, with mobile components of both leaflets of the bilayer freely diffusing over the entire surface of the substrate.

The lateral fluidity of supported membranes is a key feature that distinguishes them from other surfaces. Although fluidity provides the membrane with a variety of unique properties, it presents an intrinsic difficulty in that membrane components are continually

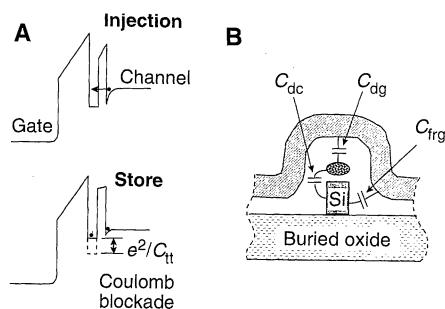


**Fig. 5.** (A) Schematic band diagram before and after injection of an electron into the dot. A single electron stored in the dot can raise its potential by  $e^2/C_{tt}$ , blocking the entry of other electrons from the channel ( $C_{tt}$  is the total capacitance of the floating gate). (B) Schematic cross section of the device showing the capacitive coupling between various elements.

J. T. Groves and S. G. Boxer, Department of Chemistry, Stanford University, Stanford, CA 94305, USA.  
N. Ulman, Department of Electrical Engineering, Edward L. Ginzton Laboratory, Stanford University, Stanford, CA 94305, USA.

\*To whom correspondence should be addressed. E-mail: SBoxer@Leland.Stanford.edu

mixing. Micropartitioning of fluid membranes allows fabrication of surfaces that preserve their distinctive properties while gaining precise control over the diffusive mixing and flow of membrane components.

Oxidized Si and fused silica ( $\text{SiO}_2$ ) wafers are suitable substrates for supported membranes (12). Standard positive photoresist (13) was spun onto wafers to a thickness of 1  $\mu\text{m}$ . The wafers were exposed to ultraviolet light through a photolithographic mask and developed. After a 3-min etch in Ar plasma, the photoresist-partitioned surfaces were ready for membrane deposition. For fabrication of  $\text{Al}_2\text{O}_3$  and Au barriers, the photoresist was exposed with the inverse mask and used as a template for lift-off of electron beam-evaporated thin films. Supported bilayers were formed by fusion of small unilamellar vesicles (diameter  $\sim 25$  nm) consisting primarily of L- $\alpha$ -phosphatidylcholine (PC) molecules doped with 1 mol% of the fluorescently labeled lipid Texas Red DHPE (14). The vesicle fusion process is quite general, accommodating a variety of lipid compositions as well as the incorporation of membrane proteins (7, 15, 16). Vesicles spontaneously assembled from solution in a matter of seconds to form a continuous single bilayer on the exposed portion of the  $\text{SiO}_2$  substrate. Excess vesicles were rinsed away while the membrane was kept under water at all times. Supported membranes were stable under water and retained their uniformity and fluidity for weeks.

Membrane-coated surfaces can be viewed directly by fluorescence microscopy and appear uniform to the diffraction-limited resolution of the microscope. A supported membrane was partitioned into an array of isolated membrane patches by micropatterned lines of photoresist (Fig. 2A). The photoresist barriers appear dark against the fluorescence from the Texas Red lipid probe in the membrane (17). These 200  $\mu\text{m}$  by 200  $\mu\text{m}$  corrals are part of a 1- $\text{cm}^2$  array of 2500 identical regions. The smallest corrals we observed were 5  $\mu\text{m}$  by 5  $\mu\text{m}$ , with 1- $\mu\text{m}$ -wide barriers (18). About 2.8 million such corrals are contained in the 1- $\text{cm}^2$  array.

Long-range fluidity within the corrals could be observed by fluorescence recovery after photobleaching. A circular spot of light was used to sequentially photobleach the fluorescent probe molecules in five individual corrals (Fig. 2B). Long-range fluidity of the membrane is indicated by the spreading of the bleached region to fill each square corral. If the membrane were not fluid, a circular bleached (dark) region would remain (19). Lines of photoresist are effective barriers to lateral diffusion, as demonstrated by their ability to confine the photobleached region of membrane within the square corral.

Bleach patterns such as those shown in Fig. 2, B and C, were stable for many days, whereas spots photobleached into membranes without any such barriers diffused away completely in about 30 min (20). The barriers shown in Fig. 2, A and B, are 10  $\mu\text{m}$  wide; those in Fig. 2C are 2  $\mu\text{m}$  wide, and the narrowest lines tested to date, 1  $\mu\text{m}$ , were equally functional as diffusion barriers (18). These results demonstrate that, within a given corral, diffusive mixing occurs as in free fluid membranes and that there is no intermixing between different corrals.

A noteworthy point is that the barriers used to confine the fluid membrane are not mechanical. Supported bilayers are highly conformal and will follow the contour of corrugated surfaces without disruption. We have deposited membranes on  $\text{SiO}_2$  substrates with topographies identical to those of the photoresist-patterned surfaces and observed no difference in lateral diffusion properties compared with flat, unpatterned  $\text{SiO}_2$  surfaces. Thus, it is the difference in the surface electrostatic and chemical properties of the substrate and barrier material that give rise to the partitioning of the membrane. We have also found that Au and  $\text{Al}_2\text{O}_3$  are effective as barrier materials. In principle, any substance that does not support fluid membranes can form an effective barrier to lateral diffusion (21). However, photoresist is the easiest material to pattern with a photomask, and nonconductive media are most convenient for electrophoretic experiments (see below).

Micropartitioned membranes are suitable substrates for further lithographic patterning. A light-directed chemical transformation (photobleaching of the fluorescent probe) can be used to selectively alter the composition of the membrane in individual corrals. Corrals were photobleached sequentially with varying exposure times to generate an array of patches with differing

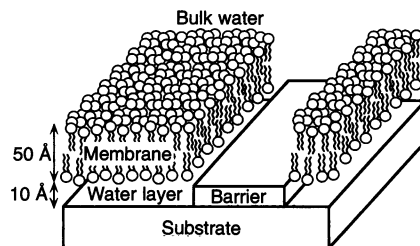


**Fig. 1.** Schematic diagram of a supported bilayer partitioned by a microfabricated barrier. The size of the membrane is exaggerated to illustrate its structure; actual membranes are typically 50 Å thick and are separated from the surface by a  $\sim 10$  Å layer of water. The height of the barriers ranged from 100 Å (Au) to 1  $\mu\text{m}$  (photoresist) with widths between 1 and 30  $\mu\text{m}$ . The functionality of a barrier depends on the surface properties of the material, not the topography.

concentrations of the fluorescent probe molecule (Fig. 2C). Because of the fluidity of the membrane, such an array can also be created with a single exposure if the area of a bleach spot is varied within individual corrals. Lateral diffusion will make the composition within each corral homogeneous in a matter of minutes. We have found that

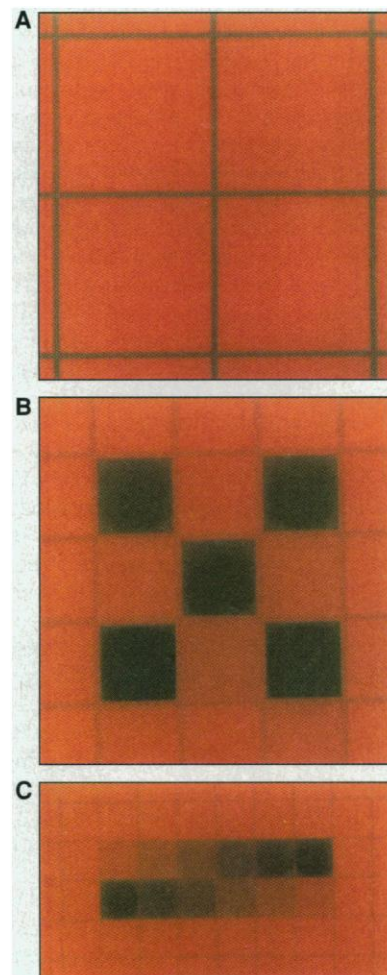


**Fig. 2.** (A) Epifluorescence photograph of four corrals (200  $\mu\text{m}$  by 200  $\mu\text{m}$ ) of a fluid, supported bilayer on an oxidized Si wafer patterned with photoresist. The photoresist barriers appear as dark lines against the bright fluorescence from the Texas Red DHPE lipid probe incorporated in the membrane. (B) An array of corrals (100  $\mu\text{m}$  by 100  $\mu\text{m}$ ) in which certain individual corrals were photobleached. Diffusive mixing of molecules within each corral has caused the circular bleached spot to spread, filling the square corral, while the photoresist barriers have prevented mixing between separate corrals (19). (C) Epifluorescence photograph of an array of corrals (50  $\mu\text{m}$  by 50  $\mu\text{m}$ , with barriers 2  $\mu\text{m}$  wide) in which certain individual corrals were selectively photobleached with varying exposure times. Corrals were exposed in increments of 30 s, with the darkest corral receiving a 3-min exposure. We created similar patterns with varying concentrations of the fluorescent probe with a single exposure by masking variable fractional areas in different corrals.

creating variable composition arrays by either of these techniques works equally well. However, the single-exposure method has the advantage of being compatible with the use of a photomask to pattern large numbers of corrals simultaneously.

Another way of creating patterns in the supported bilayer that takes advantage of both fluidity and confinement is electrophoretic redistribution of charged membrane components. When an electric field is applied parallel to the membrane, the charged molecules drift in the plane of this 2D fluid (22, 23). The PC molecules that constitute the bulk of the membrane are neutral, and thus it is expected that they will be unaffected by the field. Steady-state, electric field-induced concentration profiles (24) of the negatively charged fluorescent probe can be clearly seen to build up against the barriers in confined regions of the membrane (Fig 3, A and B).

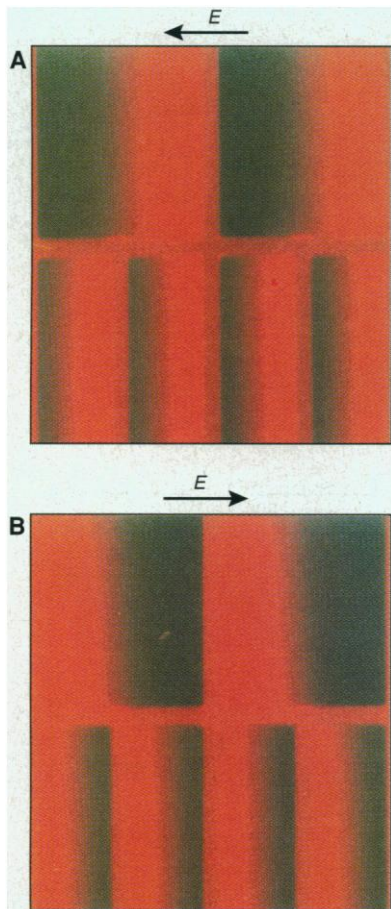


**Fig. 3.** Epifluorescence photographs of electric field ( $E$ )-induced concentration gradients of the negatively charged fluorescent probe lipid (Texas Red DHPE) in membranes confined by microfabricated corrals. Each of the upper two corrals is 200  $\mu\text{m}$  wide. Reversal of the field causes the direction of the profile to reverse. These are steady-state gradients at a field strength of 15 V/cm. The time required to switch from one direction (**A**) to the other (**B**) is  $\sim 25$  min.

Patterns of photoresist barriers are also fluorescent and appear as an intermediate shade of red in these photographs. Images of the same region with the electric field in opposite polarities are shown, demonstrating the reversibility of these profiles. At a field strength of 15 V/cm, it took  $\sim 25$  min for a steady-state concentration gradient to form in the 200- $\mu\text{m}$ -wide corrals; a complete reversal in the direction of the profile took the same amount of time. The profiles could be switched numerous times without any apparent effect on the membrane or the barriers. When the field was turned off, it took  $\sim 30$  min for gradients in the 200- $\mu\text{m}$ -wide corrals to relax back to uniformity by diffusive mixing.

The electrophoretic response can also be used to acquire physical information about the membrane in individual corrals. The profile of the steady-state gradient in dilute systems can be quantitatively described by competition between lateral diffusion and field-induced drift (24, 25). Image analysis thus provides an intrinsically parallel means of monitoring these molecular properties in numerous corrals. More complex profiles have been observed in highly concentrated domains of membrane-tethered proteins; such systems may be useful in the study of intermolecular interactions (15).

The techniques described here provide new opportunities for the study of physical and biological properties of membranes. In particular, secondary lithographic modification of the membrane could be generalized by combination with light-directed synthesis (4). Spatially addressable molecular libraries (peptide sequences, for example) could be synthesized and displayed on the surface of confined patches of fluid membrane. In some ways, this approach is analogous to phage display, except that here the peptide sequence is defined by its location in the array, thus providing immediate identification. Such libraries would be especially useful for cell screening because of the native-like surface provided by the supported membrane. For example, purified major histocompatibility complex protein incorporated into a supported membrane can effectively replace the antigen-presenting cell in the presentation of a preprocessed antigen to a helper T cell (5, 6). Other studies have underscored the similarities between supported membranes and cell surfaces by demonstrating a substantial effect from the lateral mobility of adhesion proteins in the supported bilayer on the specific binding of cells (26, 27). Additional possibilities include the construction of electrically or photochemically addressable barriers and further development of photolithographic techniques to directly change the physical, chemical, or biological properties of the fluid membrane patches.

## REFERENCES AND NOTES

- N. L. Abbott, J. P. Folkers, G. M. Whitesides, *Science* **257**, 1380 (1992).
- A. Kumar and G. M. Whitesides, *Appl. Phys. Lett.* **63**, 2002 (1993).
- Y. Xia *et al.*, *Science* **273**, 347 (1996).
- S. P. A. Fodor *et al.*, *ibid.* **251**, 767 (1991).
- H. M. McConnell, T. H. Watts, R. M. Weis, A. A. Brian, *Biochim. Biophys. Acta* **864**, 95 (1986).
- T. H. Watts and H. M. McConnell, *Annu. Rev. Immunol.* **5**, 461 (1987).
- A. A. Brian and H. M. McConnell, *Proc. Natl. Acad. Sci. U.S.A.* **81**, 6159 (1984).
- E. Sackmann, *Science* **271**, 43 (1996).
- T. M. Bayerl and M. Bloom, *Biophys. J.* **58**, 357 (1990).
- S. J. Johnson *et al.*, *ibid.* **59**, 289 (1991).
- B. W. Koenig *et al.*, *Langmuir* **12**, 1343 (1996).
- Commonly used materials known to support fluid bilayer membranes include  $\text{SiO}_2$ ,  $\text{MgF}_2$ ,  $\text{CaF}_2$ , and mica, as well as various derivatized surfaces and hydrated polymer films (8).
- Shipley S-1813 positive photoresist based on the standard diazoquinone-novolac system.
- N*-(Texas Red sulfonyl)-1,2-dihexadecanoyl-*sn*-glycerol-3-phosphoethanolamine.
- J. T. Groves, C. Wülfing, S. G. Boxer, *Biophys. J.* **71**, 2716 (1996).
- J. Salafsky, J. T. Groves, S. G. Boxer, *Biochemistry* **35**, 14773 (1996).
- The photoresist barriers are also fluorescent but appear dark against the bright background of the membrane in Fig. 2. The fluorescence intensity of the membrane in unbleached corrals decreased over time as a result of photobleaching during observation, which caused the contrast between the barriers and the membrane to vary as well.
- Electron beam lithography along with near-field scanning microscopy could be used to generate and image membrane patterns on the nanometer scale. The limiting factor at present is the resolution of the epifluorescence microscope.
- A faint shadow of the circular illumination spot can be seen remaining in Fig. 2, B and C. This is attributable to a small immobile fraction of the Texas Red DHPE probe, which can be eliminated with the use of more rigorous cleaning procedures. Soaking in piranha solution (3:1  $\text{H}_2\text{SO}_4$ - $\text{H}_2\text{O}_2$ ) or boiling in detergent (1:4 dilution of ICN 7X, for example) in addition to the etch in Ar plasma generally produces surfaces with no detectable immobile fraction. These treatments, however, necessitate the use of a more robust substance such as  $\text{Al}_2\text{O}_3$  or Au as the barrier material.
- See, for example, (16).
- The precise balance of forces governing the interaction between membranes and surfaces is not fully understood. The transparent semiconductor indium-tin oxide (ITO) is an interesting example. Vesicles spontaneously fuse with the naturally hydrophilic ITO surface, but the resulting membrane lacks long-range fluidity (16).
- M. Stelzle, R. Miehlich, E. Sackmann, *Biophys. J.* **63**, 1346 (1992).
- M.-m. Poo and K. R. Robinson, *Nature* **265**, 602 (1977).
- J. T. Groves and S. G. Boxer, *Biophys. J.* **69**, 1972 (1995).
- $C(r) = C_0 \exp(\mathbf{V} \cdot \mathbf{r} / D)$ , where  $C$  is the concentration of the charged probe molecules,  $C_0$  is the average concentration,  $D$  is the diffusion coefficient,  $\mathbf{V}$  is the field-induced drift velocity, and  $\mathbf{r}$  is the position vector.
- P.-Y. Chan *et al.*, *J. Cell Biol.* **115**, 245 (1991).
- A. Tözere *et al.*, *ibid.* **116**, 997 (1992).
- We thank H. M. McConnell, who provided helpful advice and the use of facilities in his laboratory. We also thank D. M. Bloom and G. S. Kino for support and encouragement. Supported in part by grant N00014-91-J-1050 from the Joint Services Electronics Program, the NSF Biophysics Program (S.G.B.), and NSF grant MCB-9316256 (H. M. McConnell). Processing work was carried out at the Stanford Nanofabrication Facility and was supported in part by an NSF-sponsored users grant.

16 October 1996; accepted 9 December 1996